Available online at www.sciencedirect.com

ScienceDirect

Energy Procedia 1 (2009) 1163–1169

Energy Procedia

www.elsevier.com/locate/procedia

GHGT-9

Absorption and desorption rates of carbon dioxide with monoethanolamine and piperazine

Ross Dugas[a], Gary Rochelle[a,*]

[a]*Department of Chemical Engineering, The University of Texas at Austin, 1 University Station C0400, Austin, TX 78712, USA*

Abstract

CO_2 absorption/desorption was measured in a wetted wall column at 40 and 60˚C with 7, 9, 11, and 13 m monoethanolamine (MEA) and 2, 5, 8, and 12 m piperazine (PZ) at various CO_2 loadings. 8 m PZ has about a 75% greater CO_2 capacity than 7 m MEA. CO_2 absorption and desorption is 2–3 times faster with PZ than with MEA at equivalent CO_2 partial pressure. The CO_2 flux normalized by the liquid side partial pressure driving force, k_g', for both MEA and PZ is practically independent of temperature and amine concentration over the range of these experiments when represented as a function of the equilibrium partial pressure at 40˚C. Normalized flux decreases a factor of 10 as the equilibrium partial pressure at 40˚C increases from 100 to 10000 Pa

Keywords: carbon dioxide; monoethanolamine; piperazine; absorption; desorption; rates; partial pressure; capacity

1. Introduction

CO_2 absorption and desorption rates are important in CO_2 capture since they can affect both capital and operating costs. Faster solvents can reduce the amount of packing required in the absorber and stripper and can also achieve a closer approach to equilibrium in the absorber, saving energy in the stripper.

CO_2 absorption rates into highly loaded, highly concentrated monoethanolamine (MEA) solutions have been measured by Aboudheir [1] and Dang [2]. Absorption rates in CO_2 loaded dilute piperazine (PZ) have been measured by Bishnoi [3]. CO_2 partial pressures in loaded MEA and PZ solutions at absorber temperatures have been measured by Hilliard [4], Jou [5], Dang [2], Bishnoi [3] and Ermatchkov [6].

Carbon dioxide absorption and desorption rates for 7, 9, 11, and 13 m MEA and 2, 5, 8, and 12 m PZ were measured in a wetted wall column at 40 and 60˚C. For each amine concentration about 4 CO_2 loadings were tested. The CO_2 loadings represent the expected range of CO_2 loading in a CO_2 capture system for a coal-fired power plant. The equilibrium CO_2 partial pressure and liquid film mass transfer coefficients were measured at each condition.

2. Experimental Apparatus

The wetted wall column countercurrently contacts an aqueous amine solution with N_2/CO_2 on the surface of a stainless steel rod with a known surface area. Several researchers (Cullinane [7], Al-Juaied [8], Bishnoi [3], Dang [2]) have made rate and CO_2

* Corresponding author. Tel.: 512-471-7230; fax: 512-471-7060
E-mail address: gtr@che.utexas.edu.

doi:10.1016/j.egypro.2009.01.153

partial pressure measurements with this equipment. A schematic of the overall wetted wall column is shown in Figure 1. A more detailed view of the reaction chamber is shown in Figure 2.

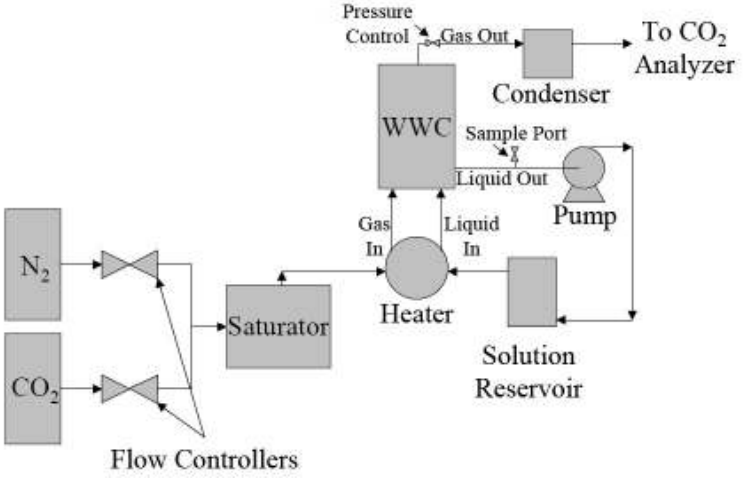

Figure 1. Schematic of the Wetted Wall Column

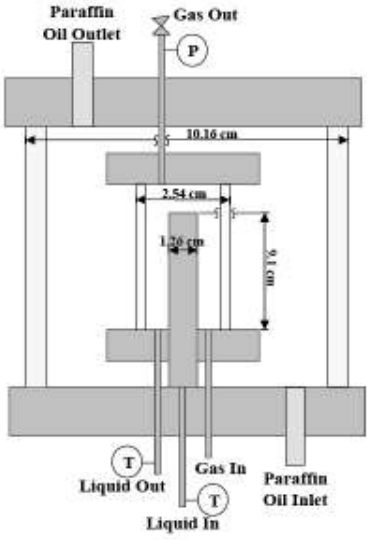

Figure 2. Schematic of the Wetted Wall Column Reaction Chamber

Nitrogen and carbon dioxide are mixed using mass flow controllers to create a simulated flue gas of known concentration. The gas is saturated and heated at the experimental temperature before entering the wetted wall column reaction chamber. In the chamber the gas countercurrently contacts the falling amine solution film on the surface of the stainless steel rod. CO_2 is either absorbed or desorbed into the gaseous phase. The outlet flue gas is dried using a condenser and $CaSO_4$ desiccant. The dry flue gas is analyzed by a Horiba CO_2 analyzer accurate to 0.5% of full scale. The Horiba analyzers have ranges of 0–500, 1000, 5000 ppm and 0–1, 2, 10, 20 mol%. Since the flow rate of gas, inlet and outlet CO_2 concentrations and contact area for reaction are known, the flux and resultant kinetics can be determined. By testing inlet CO_2 concentrations that result in absorption and desorption, the equilibrium partial pressure can be bracketed and determined.

The wetted wall column can be operated from atmospheric pressure up to 100 psig, or 7 atmospheres gauge. Gas and liquid flow rates are typically 4–6 standard L/min and 0.18–0.24 L/min, respectively.

3. Results and Discussion

CO_2 absorption and desorption experiments in the wetted wall column are conducted using 6 inlet CO_2 partial pressures for each solvent condition. The flux of CO_2 is directly related to the log mean CO_2 partial pressure driving force, assuming plug flow for the gas. The equilibrium partial pressure is obtained by iterating to the zero flux partial pressure. The slope of the curve fitted line is equal to the overall mass transfer coefficient K_G. The overall mass transfer coefficient can be converted to the liquid film mass transfer coefficient, k_g', by using the series resistance relationship (Equation 1) and a correlation [9] for the gas film mass transfer coefficient, k_g. Each set of 6 CO_2 absorption or desorption experiments, as shown in Figure 3, results in one k_g' value. Obtained k_g' values are a function of both the reaction kinetics and the diffusion of reactants and products, characterized by k_l^o. The k_g' rate plots (Figures 7–9) include physical mass transfer resistance. k_l^o estimations [9] are included in Tables 1 and 2. The diffusion coefficient of CO_2 in solution is calculated via the N_2O analogy. Diffusion coefficients in water were obtained from Versteeg [10]. N_2O diffusion rates in amines were obtained from Cullinane [9].

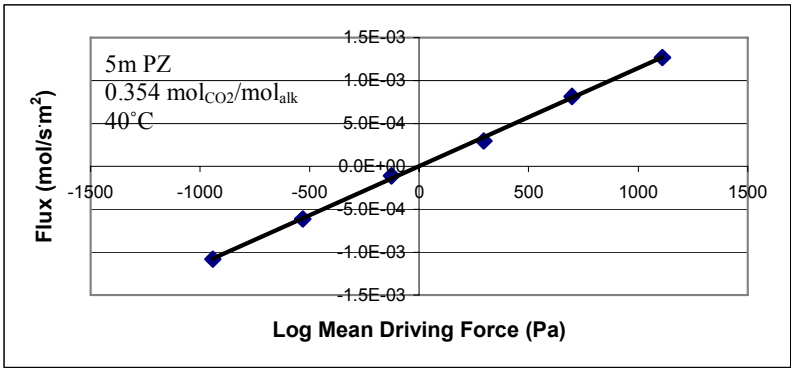

Figure 3. Flux-Driving Force Dependence for 5 m PZ, 0.354 mol_{CO2}/mol_{alk}, 40˚C

$$\frac{1}{K_G} = \frac{1}{k_g} + \frac{1}{k_g'} \quad (1)$$

The measured CO_2 partial pressure and rate data for MEA and PZ are listed in Tables 1 and 2, which include loaded amine solutions at expected conditions for CO_2 capture from coal-fired power plants. All experimental runs are less than 50% gas film controlled. 12 m PZ solution was too viscous at 40˚C to use in the wetted wall column. 12 m PZ near 0.4 loading at 60°C was not tested because of solid precipitation.

Table 1. CO_2 Partial Pressure and Rate Data for 7, 9, 11, and 13 m MEA Solutions at 40 and 60˚C

MEA	Temp	CO_2 Loading	P_{CO2}	Q_{Liq}	k_l^o	k_g'
m	C	mol/mol_{alk}	Pa	mL/s	m/s	$mol/s \cdot Pa \cdot m^2$
7	40	0.252	15.7	3.2	7.5E-05	3.34E-06
		0.351	77	3.2	6.4E-05	1.40E-06
		0.432	465	3.1	6.3E-05	7.66E-07
		0.496	4216	3.1	6.5E-05	3.47E-07
	60	0.252	109	3.2	9.0E-05	2.92E-06
		0.351	660	3.2	8.0E-05	1.70E-06
		0.432	3434	3.1	7.9E-05	9.28E-07
		0.496	16157	3.1	7.9E-05	3.76E-07
9	40	0.231	10.4	3.3	7.2E-05	-
		0.324	34	3.1	6.3E-05	1.86E-06
		0.382	107	3.1	6.1E-05	1.40E-06
		0.441	417	3.1	5.9E-05	8.36E-07
		0.496	5354	3.0	5.9E-05	3.02E-07
	60	0.231	61	3.3	8.3E-05	3.80E-06
		0.324	263	3.1	7.7E-05	2.44E-06
		0.382	892	3.1	7.4E-05	1.47E-06
		0.441	2862	3.1	7.3E-05	9.57E-07
		0.496	21249	3.0	7.0E-05	3.24E-07

MEA	Temp	CO_2 Loading	P_{CO2}	Q_{Liq}	k_l^o	k_g'
m	C	mol/mol_{alk}	Pa	mL/s	m/s	$mol/s \cdot Pa \cdot m^2$
11	40	0.261	14.0	3.2	6.0E-05	3.36E-06
		0.353	67	3.1	5.5E-05	1.76E-06
		0.428	434	3.1	5.2E-05	7.14E-07
		0.461	1509	3.1	5.1E-05	4.34E-07
	60	0.261	96	3.2	7.4E-05	3.35E-06
		0.353	634	3.1	6.7E-05	1.80E-06
		0.428	3463	3.1	6.4E-05	8.71E-07
		0.461	8171	3.1	6.3E-05	5.02E-07
13	40	0.252	12.3	3.2	5.4E-05	3.08E-06
		0.372	84	2.7	4.7E-05	1.28E-06
		0.435	491	3.1	4.7E-05	6.96E-07
		0.502	8792	3.1	4.5E-05	1.62E-07
	60	0.252	100	2.7	6.4E-05	2.98E-06
		0.372	694	2.7	5.8E-05	1.54E-06
		0.435	3859	3.1	5.7E-05	7.56E-07
		0.502	29427	2.9	5.5E-05	1.93E-07

Table 2. CO_2 Partial Pressure and Rate Data for 2, 5, 8, and 12 m PZ Solutions at 40 and 60˚C

PZ	Temp	CO_2 Loading	P_{CO2}	Q_{Liq}	k_l^o	k_g'
m	C	mol/mol_{alk}	Pa	mL/s	m/s	$mol/s \cdot Pa \cdot m^2$
2	40	0.240	96	3.0	9.0E-05	3.32E-06
		0.316	499	3.0	9.0E-05	2.04E-06
		0.352	1305	3.0	8.9E-05	1.39E-06
		0.411	7127	3.0	9.0E-05	5.55E-07
	60	0.240	559	3.0	1.1E-04	3.33E-06
		0.316	2541	3.0	1.1E-04	2.06E-06
		0.352	5593	3.0	1.1E-04	1.38E-06
		0.411	25378	3.0	1.0E-04	3.84E-07
5	40	0.226	65	3.6	6.0E-05	4.39E-06
		0.299	346	3.6	5.7E-05	2.57E-06
		0.354	1120	3.5	5.4E-05	1.69E-06
		0.402	4563	3.5	5.3E-05	7.93E-07
	60	0.226	385	3.6	7.4E-05	4.75E-06
		0.299	1814	3.6	7.0E-05	2.62E-06
		0.354	5021	3.5	6.6E-05	1.80E-06
		0.402	17233	3.3	6.2E-05	6.59E-07

PZ	Temp	CO_2 Loading	P_{CO2}	Q_{Liq}	k_l^o	k_g'
m	C	mol/mol_{alk}	Pa	mL/s	m/s	$mol/s \cdot Pa \cdot m^2$
8	40	0.231	68	4.0	3.8E-05	4.27E-06
		0.305	530	3.1	3.5E-05	1.98E-06
		0.360	1409	3.7	3.7E-05	1.14E-06
		0.404	8153	3.7	3.6E-05	3.53E-07
	60	0.231	430	3.5	5.1E-05	4.41E-06
		0.305	2407	3.1	4.7E-05	2.02E-06
		0.360	7454	3.5	4.7E-05	9.57E-07
		0.404	30783	3.7	4.6E-05	3.20E-07
12	60	0.231	331	4.0	3.6E-05	4.19E-06
		0.289	1865	3.9	3.4E-05	1.85E-06
		0.354	6791	3.9	3.1E-05	7.73E-07

Figure 4 shows the comparison of the obtained CO_2 partial pressure data with literature values for MEA solutions at 40 and 60˚C. Both Hilliard [4] and Jou [5] used equilibrium cell that recirculate the gas phase through the amine solvent to achieve equilibrium. The filled points represent the CO_2 partial pressures obtained using the wetted wall column from each series of 6 absorption or desorption runs.

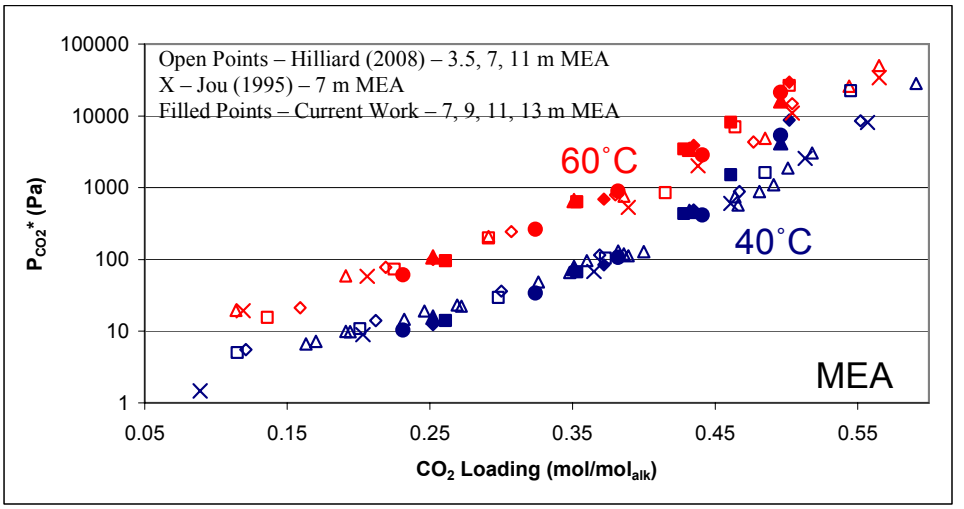

Figure 4. CO_2 Partial Pressure Data for Monoethanolamine Solutions at 40 and 60˚C

Below 0.45 loading the data with our wetted wall column match the data of Hilliard [4] and Jou [5]. However, above 0.45 loading the new data are higher and seem to be a function of amine concentration.

The measured CO_2 partial pressure in piperazine solution is comparable to the results of Hilliard [4] and Ermatchkov [6] (Figure 5).

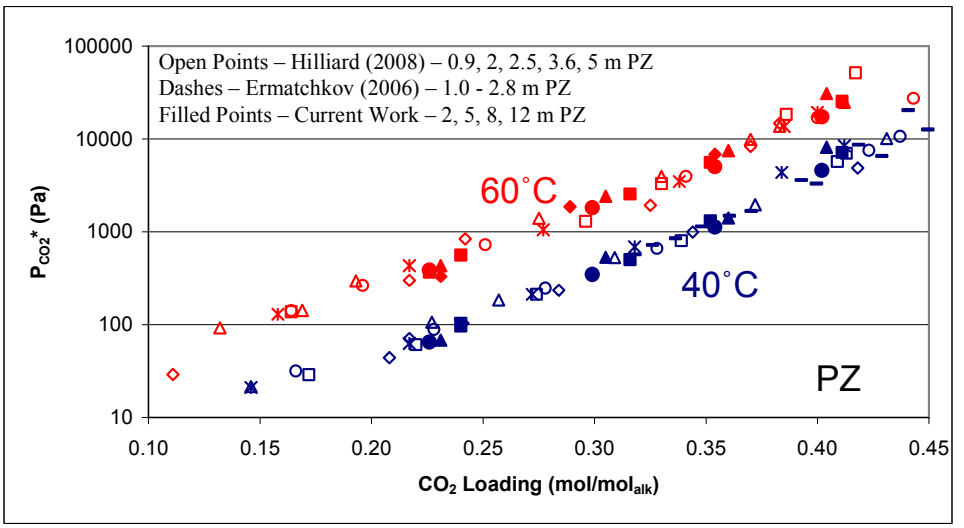

Figure 5. CO_2 Partial Pressure for Piperazine Solutions at 40 and 60˚C

When represented as a function of CO_2 loading the equilibrium CO_2 partial pressure of both MEA and PZ solutions is not a function of amine concentration. Therefore more concentrated solution will always have a greater CO_2 capacity. In an absorption/stripping process solvent compositions with greater capacity will result in lower solvent flow rates and likely significant energy savings due to a reduction in the sensible heat energy requirement in the stripper.

Figure 6 shows the working capacity for CO_2 as moles CO_2/(kg H_2O+amine), which will be most directly related to the sensible heat requirement. Heat capacity data [4] as well as empirical pilot plant data suggest that the presence of CO_2 does not affect the heat capacity. The CO_2 capacity is based on the difference in the CO_2 solubility between the lean and rich solutions of the absorber. Figure 6 assumes a rich solution with an equilibrium partial pressure of 5 kPa at 40˚C which is representative of approximately 40% approach to equilibrium with an inlet coal fired flue gas. Figure 6 gives capacity as a function of the partial pressure of CO_2 at the lean loading, which would depend on stripper design and optimization.

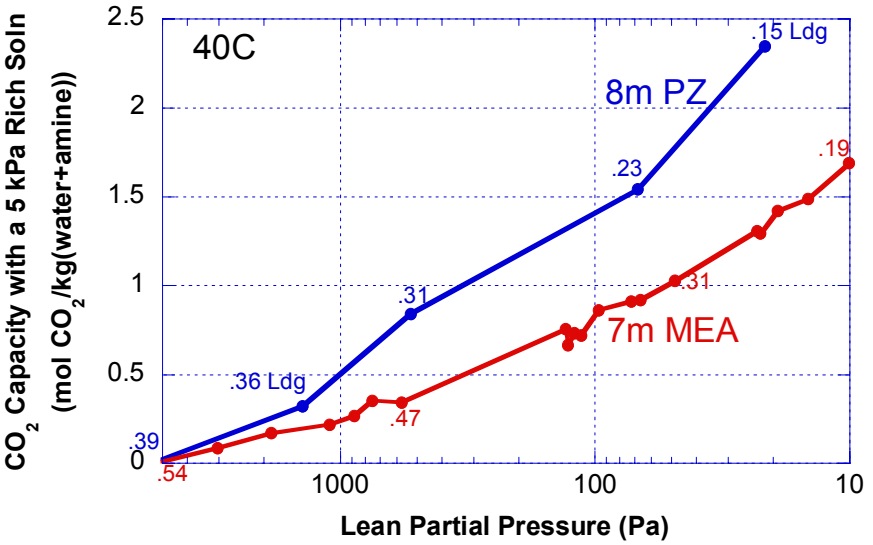

Figure 6. CO_2 Capacity of 8 m PZ and 7 m MEA at 40˚C, Assuming a 5 kPa rich Solution

Regardless of the selected lean CO_2 partial pressure, 8 m PZ seems to demonstrate an approximately 75% increase in the CO_2 capacity over 7 m MEA. This increase is mostly due to the greater amine concentration and the fact that piperazine has 2 active amines groups per molecule.

In this paper CO_2 mass transfer rates are reported as the flux divided by the liquid side driving force in partial pressure, k_g' (Equation 2). k_g' is the liquid film mass transfer coefficient in gas film units. It is expected that mass transfer rates in these systems will be dominated by the mechanism of pseudo-first order reaction with diffusion in the boundary layer given by Equation 3.

$$Flux = k_g^{'}(P_{CO2,\text{int}erface} - P^{*}_{CO2,bulk}) \quad (2)$$

$$k_g^{'} \approx \frac{\sqrt{k_2[Am]D_{CO2}}}{H_{CO2}} \quad (3)$$

The k_g' basis simplifies rate comparisons by reporting the mathematically obtained group of terms as an effective mass transfer coefficient. Henry's constant, H_{CO2}, increases with temperature [10] and amine concentration [11]. The diffusion coefficient, D_{CO2}, increases with temperature and decreases with amine concentration. The concentration of free amine will increase with amine concentration. The rate constant will increase with temperature and may also be a function of the ionic strength environment.

The results from the wetted wall column suggest that when k_g' is represented as a function of the P_{CO2} (or CO_2 loading) at 40˚C, k_g' does not depend on temperature or amine concentration. This empirical result suggests that the parameters in Equation 2 vary in such a way that their individual variance with temperature and amine concentration cancel.

The lack of temperature dependence on k_g' can be seen in Figure 7 which compares the current work at 7 m MEA to data obtained by Aboudheir [1] and Dang [2].

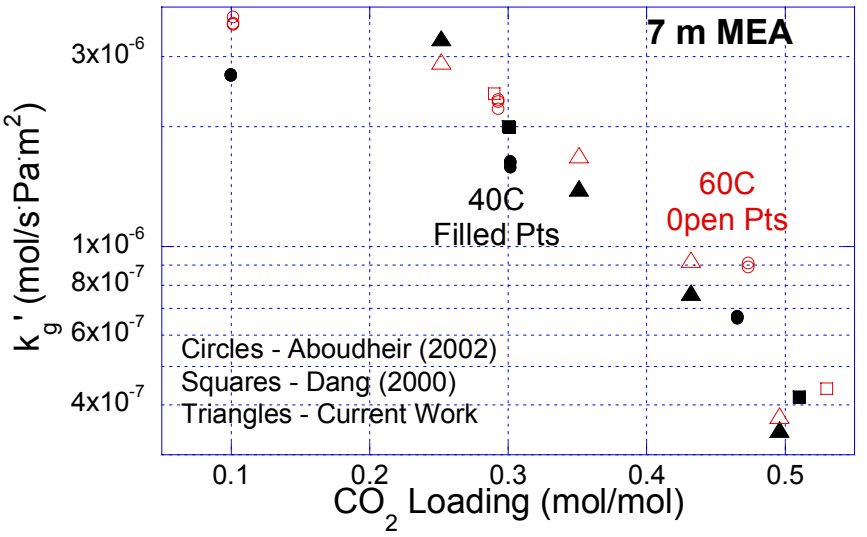

Figure 7. CO_2 Absorption Rate Data for 7 m MEA at 40 and 60˚C

Aboudheir used a laminar jet absorber. Dang used the same wetted wall column as in this work. The diffusion of reactants and products may explain why Aboudheir data at low loading do not follow the trend.

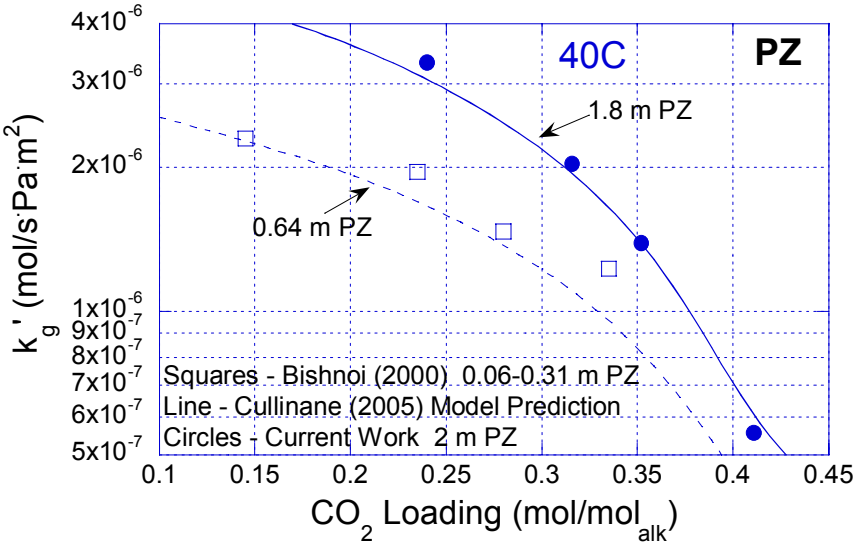

Figure 8. CO_2 Absorption Data for Piperazine at 40˚C.

Figure 8 compares 2 m PZ data to very dilute piperazine data obtained by Bishnoi [3]. These points probably fall below 2 m PZ since the amine concentration is so low. The predicted 0.64 and 1.8 m PZ rate curves by Cullinane use rate constants determined by the regression of K^+/PZ data [9].

Figure 9 plots k_g' versus the equilibrium partial pressure of the solution at 40˚C to show that temperature and the amine concentration do not significantly affect k_g' values for MEA or PZ solutions at 40 and 60˚C. For both MEA and PZ solutions, k_g' is reduced drastically with an increase in equilibrium partial pressure, representative of CO_2 loading. This is mostly due to a decrease in free amine at higher CO_2 loading. CO_2 reaction rates for PZ are about 2–3 times faster than with MEA at comparable CO_2 partial pressures. The 12 m PZ points at 60˚C are not included in Figure 9 since the equilibrium partial pressures of the solutions were not able to be verified at 40˚C due to viscosity limitations.

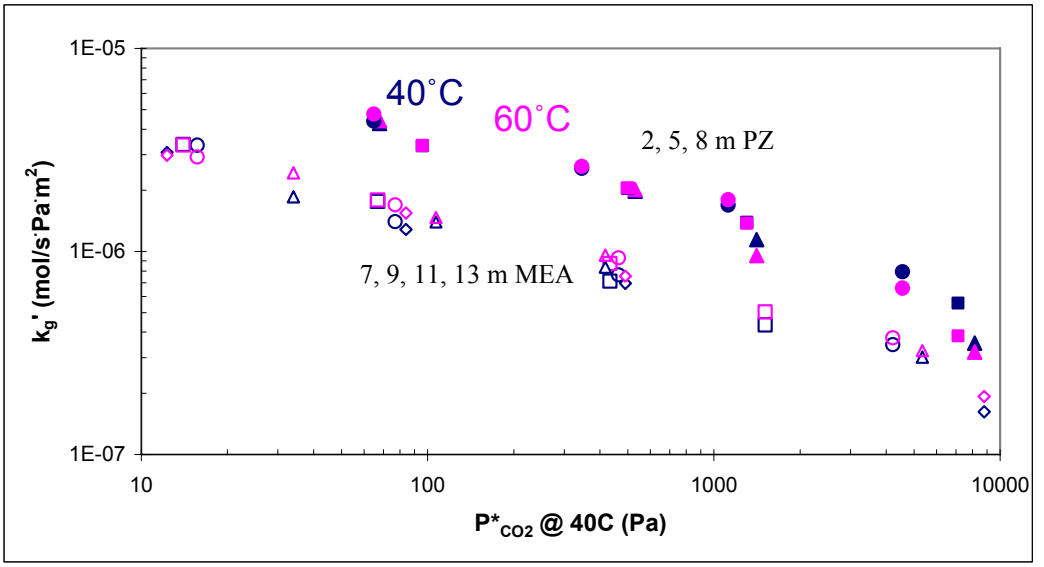

Figure 9. Absorption/Desorption Rates for CO_2 in MEA and PZ Solutions Plotted Versus the Equilibrium Partial Pressure at 40˚C

Since k_g' is essentially independent of amine concentration, more concentrated amine solutions should have lower energy requirements for CO_2 capture. Corrosion, degradation, viscosity, solubility, packing wetting or heat transfer concerns could limit the amine concentration in industrial operation.

4. Conclusions

CO_2 partial pressure and rate data from MEA and PZ wetted wall column experiments agreed very well with literature values. CO_2 partial pressure data for MEA solutions showed a small deviation at loadings higher than 0.45. Rate variations from literature reported values can be explained by mass transfer phenomenon.

8 m PZ has about a 75% greater operational CO_2 capacity than 7 m MEA. CO_2 reaction rates for PZ were shown to be 2–3 times faster than MEA solutions. Despite the fact that k_g' incorporates terms which are strongly temperature and amine concentration dependent, k_g' is essentially independent of temperature and amine concentration at 40 and 60˚C.

5. References

1. A.A. Aboudheir (2002). Kinetics, Modeling, and Simulation of Carbon Dioxide Absorption into Highly Concentrated and Loaded Monoethanolamine Solutions. Chemical Engineering. Regina, Saskatchewan, Canada, University of Regina. Ph.D.: 364.
2. H. Dang and G.T. Rochelle (2003). "CO_2 Absorption Rate and Solubility in Monoethanolamine/Piperazine/Water," *Separation Sci & Tech,* 38(2): 337–357.
3. S. Bishnoi and G.T. Rochelle (2000). "Absorption of Carbon Dioxide into Aqueous Piperazine: Reaction Kinetics, Mass Transfer and Solubility." *Chem. Engr. Sci*, 55: 5531–5543.
4. M.D. Hilliard (2008). A Predictive Thermodynamic Model for an Aqueous Blend of Potassium Carbonate, Piperazine, and Monoethanolamine for Carbon Dioxide Capture from Flue Gas. Chemical Engineering. Austin, The University of Texas at Austin. Ph.D.: 1025.
5. F.-Y. Jou, A.E. Mather, *et al.* (1995). "The Solubility of CO_2 in a 30 Mass Percent Monoethanolamine Solution." *Can. J. Chem. Eng*, 73(1): 140–147.
6. V. Ermatchkov, A. Perez-Salado Kamps, *et al.* (2006). "Solubility of Carbon Dioxide in Aqueous Solutions of Piperazine in the Low Gas Loading Region." *J. Chem. & Eng. Data,* 51(5): 1788–1796.
7. J.T. Cullinane and G.T. Rochelle (2006). "Kinetics of Carbon Dioxide Absorption into Aqueous Potassium Carbonate and Piperazine." *Ind. & Eng. Chem. Res,* 45(8): 2531–2545.
8. M. Al-Juaied and G.T. Rochelle (2006). "Absorption of CO_2 in Aqueous Blends of Diglycolamine and Morpholine." *Chem. Eng. Sci,* 61(12): 3830–3837.
9. J.T. Cullinane (2005). Thermodynamics and Kinetics of aqueous piperazine with potassium carbonate for carbon dioxide absorption. Chemical Engineering. Austin, TX, The University of Texas at Austin: 295.
10. G.F. Versteeg, L.A.J. Van Dijck, *et al.* (1996). "On the Kinetics Between CO_2 and Alkanolamines Both in Aqueous and Non-aqueous Solutions. An Overview." *Chem. Eng. Comm*, 144: 113–158.
11. G.J. Browning and R.H. Weiland (1994). "Physical Solubility of Carbon Dioxide in Aqueous Alkanolamine via Nitrous Oxide Analogy." *J. Chem. & Eng. Data*, 39: 817–822.